Journal of Materials Chemistry A

RSC Publishing

COMMUNICATION

View Article Online
View Journal | View Issue

Cite this: *J. Mater. Chem. A*, 2013, **1**, 12422

Received 9th July 2013
Accepted 29th August 2013

DOI: 10.1039/c3ta12663c

www.rsc.org/MaterialsA

Winding ultrathin, transparent, and electrically conductive carbon nanotube sheets into high-performance fiber-shaped dye-sensitized solar cells†

Hao Sun, Xiao You, Zhibin Yang, Jue Deng and Huisheng Peng*

Highly aligned carbon nanotube sheets, that are transparent, flexible, and electrically conductive, have been wrapped onto a modified titanium wire to produce novel, fiber-shaped dye-sensitized solar cells. The designed coaxial structure offers a high energy conversion efficiency and stability during the deformation.

Compared with silicon-based solar cells, dye-sensitized solar cells (DSCs) can be made into flexible, thin devices with promising applications that remain difficult for rigid silicon wafers.[1–6] However, the planar structure cannot adequately meet the ongoing requirement for small and rapid electronic devices in the future. To this end, if DSCs could be made in a flexible, coaxial fiber format, they might be lightweight and efficient for many promising applications over the conventional planar cells.[7–9] For instance, they can be easily integrated into micro-devices and woven into electronic textiles, which is required in electronics. In this case, it is critical but remains challenging to find appropriate counter electrode materials. A good candidate needs to be flexible, robust, transparent, conductive, stable, and electrocatalytic to the redox couple.

In this work, highly aligned multi-walled carbon nanotube (MWCNT) sheets are developed as a new family of materials for the counter electrodes to fabricate DSC fibers (Fig. 1). The thin MWCNT sheet is transparent, flexible, and robust. Due to the highly aligned structure of MWCNTs, the sheet is also mechanically strong, electrically conductive, and active in catalyzing the redox couple of I^-/I_3^-. Aligned TiO_2 nanotubes that are perpendicularly grown on a Ti wire have been used as a working electrode, and the MWCNT sheet is continuously wrapped around the modified Ti wire to produce a fiber-shaped DSC. The resulting photovoltaic fiber achieves a maximal energy conversion efficiency of 4.10%.

Aligned TiO_2 nanotubes are grown on a Ti wire by an electrochemical anodizing method (Fig. 2a and b). Aligned TiO_2 nanotubes with a uniform diameter of ~150 nm and wall thickness of ~20 nm have been produced (Fig. 2c). The aligned MWCNT sheet was pulled out of a spinnable MWCNT array that is described in the ESI.† The MWCNTs are highly aligned to enable electrical conductivities on the level of 10^2 to 10^3 S cm^{-1} along the MWCNT-alignment direction (Fig. 2d). The MWCNT sheet can be uniformly wrapped around the working electrode with a thickness of appropriately 20 nm (Fig. 2e). The aligned MWCNTs are closely attached at the tips of TiO_2 nanotubes (Fig. 2f).

TiO_2 nanotubes with increasing lengths from 10, 19, 31, and 39 μm have been investigated for photovoltaic fibers (Fig. 3a). The MWCNT sheets shared the same thickness of 20 nm if not specified. The open circuit voltage (V_{OC}) and fill factor (FF) are maintained to be appropriately 0.72 V and 0.580, respectively, while the short circuit current (J_{SC}) is increased from 3.61 to 9.93 mA cm^{-2} with the increasing length from 10 to 31 μm and then decreased to 8.53 mA cm^{-2} with the further increase to 39 μm (Table 1). Longer TiO_2 nanotubes can absorb more dye molecules to generate higher photoelectron currents under the

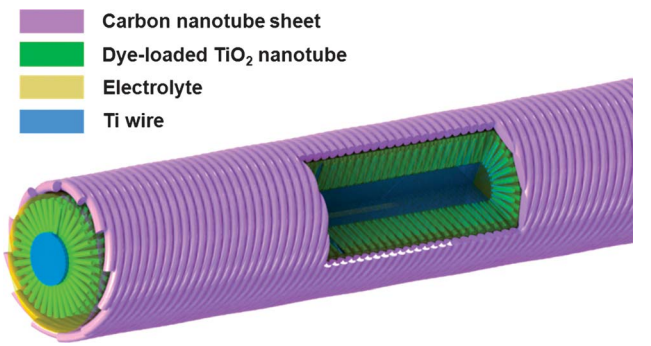

Fig. 1 Schematic illustration of the coaxial DSC fiber.

State Key Laboratory of Molecular Engineering of Polymers, Department of Macromolecular Science, Laboratory of Advanced Materials, Fudan University, Shanghai 200438, China. E-mail: penghs@fudan.edu.cn

† Electronic supplementary information (ESI) available. See DOI: 10.1039/c3ta12663c

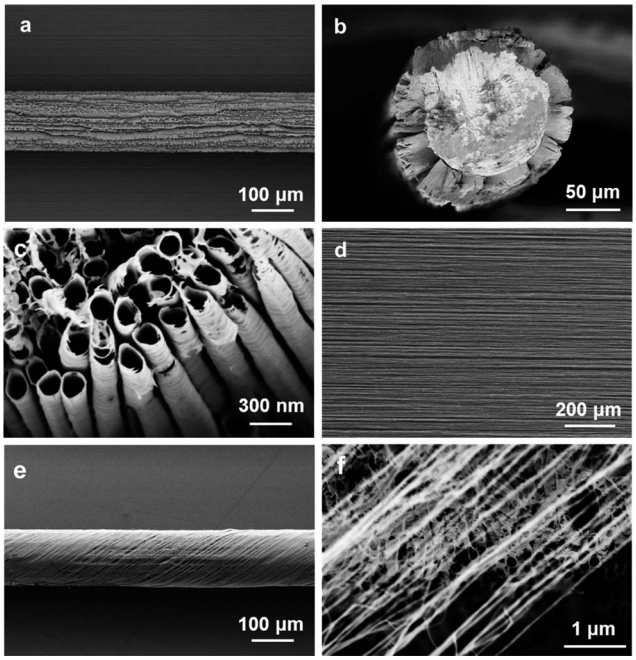

Fig. 2 Scanning electron microscopy (SEM) images of the coaxial photovoltaic fiber. (a and b) A TiO_2 nanotube-modified Ti wire: side and top views, respectively. (c) TiO_2 nanotubes at high magnification. (d) Highly aligned MWCNT sheet. (e and f) The modified Ti wire being wrapped in a layer of MWCNT sheet at low and high magnifications, respectively.

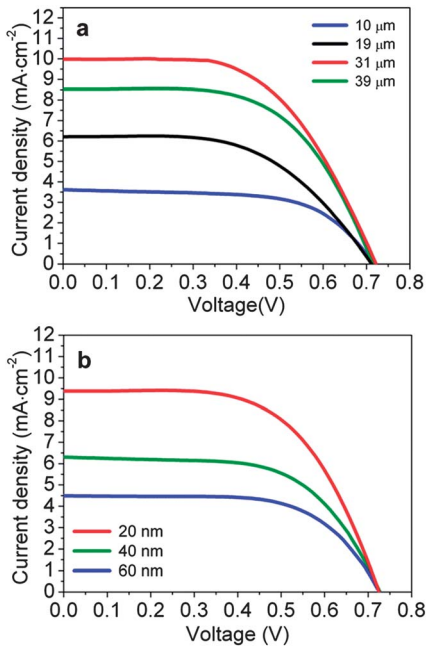

Fig. 3 (a) *J–V* curves of coaxial DSC fibers with different lengths of TiO_2 nanotubes. (b) *J–V* curves of coaxial DSC fibers with different thicknesses of MWCNT sheets.

same illumination. However, the recombination of charges becomes dominating due to the longer diffusion length of photons and electrons with the further increasing length of TiO_2 nanotubes, which reduces the collection of electrons.[10]

Different thicknesses of MWCNT sheets, *i.e.*, 20, 40, and 60 nm, have been also compared for the photovoltaic fiber (Fig. 3b). Here the length of TiO_2 nanotubes was the same, 31 μm. Both V_{OC} and FF are maintained at appropriately 0.72 V and 0.60, respectively, while the J_{SC} is continuously decreased due to the increased shield effect by the thicker MWCNT sheets (Table 2). The thicker the MWCNT sheets are, the less the incident light can reach to sensitize the dye with the lower photoelectron current (Fig. S1†).[11]

To demonstrate the high performance of the coaxial structure, a DSC wire is fabricated by winding an aligned MWCNT fiber that has been twisted from the same MWCNT sheet as the counter electrode onto the same TiO_2 nanotube-modified Ti wire (Fig. S2† and 4a). As expected, they exhibit the same V_{OC} of 0.72 V that is determined by the energy level of the electrode, N719 dye, and electrolyte.[12,13] The coaxial DSC fiber shows a lower J_{SC} than the twisted DSC wire due to the fact that a MWCNT fiber shows higher conductivity than a MWCNT sheet (typically about five times), so more photoelectrons can be transported to the external circuit. However, the coaxial DSC shows a FF of 0.570 that is much higher than 0.375 of the twisted DSC wire as the coaxial structure produces a much larger contact area between the working and counter electrodes with a higher catalytic activity. As a result, the DSC fiber exhibits a maximal energy conversion efficiency of 4.10%, compared with 3.20% of the twisted DSC wire.

Besides the much improved energy conversion efficiency, the coaxial DSC fiber also shows a higher flexibility than the twisted DSC wire. The photovoltaic parameters had been compared after bending for 100 cycles (Fig. S3† and 4b). For the coaxial DSC fiber, the J_{SC} is first slightly increased in the first 10 cycles due to an increased contact between the electrolyte and MWCNT sheet and then slightly decreased in the following 90 cycles. The energy conversion efficiency remains almost unchanged during the studied bending cycles (with a variation of less than 5%). In contrast, for the twisted DSC wire, the J_{SC} is quickly decreased by 19.5% in the first 10 cycles and further decreased by 26.9% in the following 90 cycles. As a result, the energy conversion efficiency is decreased by ~30%.

To better understand the different stabilities, the coaxial and twisted DSCs are further studied by scanning electron microscopy. Fig. 5a and b have compared the coaxial DSC fiber before and after bending for 10 cycles, and no obvious damage in the structure is observed. Therefore, the energy conversion efficiency remains almost unchanged during the bending. In contrast, the two fiber electrodes are separated from each other in a twisted DSC wire during the bending (Fig. 5c and d). The increased diffusion length for I^- ions slows the regeneration rate of the dye and makes the photoelectron recombination with I_3^- ions in the electrolyte more frequent. As a result, the J_{SC} of the twisted DSC wire is largely decreased after bending. These coaxial DSC fibers also show many other unique advantages. For instance, the energy conversion efficiency of the DSC fiber is independent of the incident angle (Fig. 6). The photovoltaic parameters remain unchanged with increasing incident angle from 0 to 180°.

Table 1 Photovoltaic parameters of DSC fibers based on different lengths of TiO_2 nanotubes

Length of TiO_2 nanotubes (μm)	V_{OC} (V)	J_{SC} (mA cm^{-2})	FF	η (%)
10	0.717	3.613	0.615	1.59
19	0.712	6.208	0.560	2.47
31	0.722	9.980	0.570	4.10
39	0.715	8.526	0.586	3.57

Table 2 Photovoltaic parameters of DSC fibers based on different thicknesses of MWCNT sheets

Thickness of MWCNT sheet (nm)	V_{OC} (V)	J_{SC} (mA cm^{-2})	FF	η (%)
20	0.722	9.378	0.596	4.03
40	0.726	6.304	0.610	2.79
60	0.722	4.479	0.641	2.07

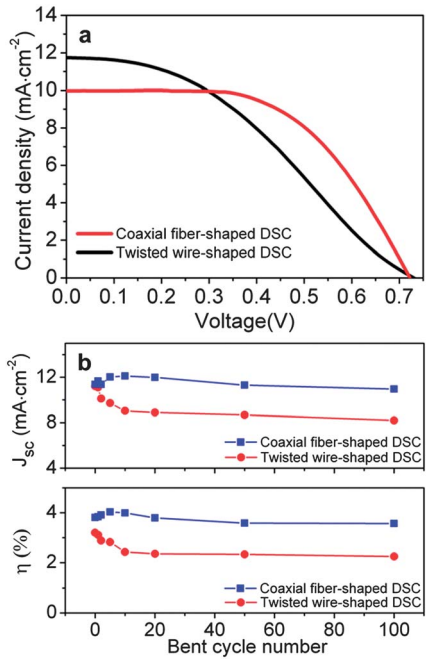

Fig. 4 (a) *J–V* curves of the coaxial DSC fiber and twisted DSC wire. (b) Dependence of photovoltaic parameters on bent cycle number for the coaxial DSC fiber and twisted DSC wire.

In summary, a new coaxial DSC fiber has been fabricated with a highly aligned MWCNT sheet as the counter electrode, and a record energy conversion efficiency of 4.10% is achieved. The coaxial DSC fiber also shows a high flexibility and stability. More efforts are under way to improve wire-shaped DSCs by introducing the other metal oxide materials.[14] Although a fiber-shaped DSC has been demonstrated in this work, the aligned MWCNT sheet can be also used as an electrode material to fabricate coaxial, fiber-shaped polymer solar cells and various other optoelectronic and electronic devices.

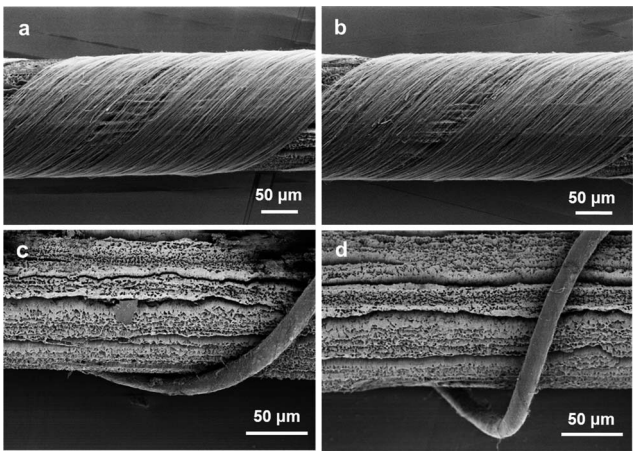

Fig. 5 Morphology characterization of (a and b) a coaxial DSC fiber and (c and d) a twisted DSC wire before and after bending for 10 cycles, respectively.

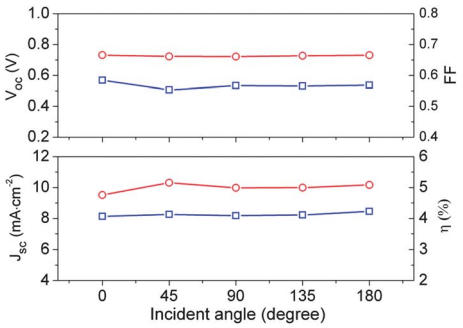

Fig. 6 Dependence of photovoltaic parameters on incident angle of a coaxial DSC fiber.

Experimental section

Ti wires with a diameter of 127 μm were sequentially immersed in acetone, isopropanol, and water to wash away impurities, and aligned TiO_2 nanotubes were grown on the surface of the Ti wire by electrochemical anodization. A 0.3 wt% NH_4F–8 wt% H_2O–ethylene glycol solution served as the electrolyte, and a voltage of 60 V was conducted between the Ti wire and Pt sheet as anode and cathode, respectively. The lengths of TiO_2 nanotubes can be controlled by varying the oxidation time. Deionized water was used to remove the residual electrolyte on the surface of the TiO_2 nanotube-modified Ti wire, followed by heating to 500 °C for 1 h and annealing in air. After the treatment in a 40 mM $TiCl_4$ aqueous solution at 70 °C for 30 min, the wire was heated to 450 °C for 30 min and annealed in air. When the temperature was dropped to ~120 °C, the resulting wire was immersed in 0.3 mM N719 solution in a mixture of dehydrated acetonitrile and *tert*-butanol (volume ratio of 1/1) for 16 h prior to the device fabrication.

Spinnable MWCNT arrays were synthesized by chemical vapor deposition.[15] A transparent, conductive MWCNT sheet could be pulled out of a spinnable CNT array with a razor blade with a single edge, and it was then carefully wrapped around the modified Ti wire. For the twisted structure, the MWCNT sheets were spun into fibers with a rotation rate of 2000 rpm to function

as a counter electrode. The DSC fiber and wire were sealed by transparent fluorinated ethylene propylene tubes, followed by injection of the electrolyte (0.05 M iodine, 0.1 M lithium iodide, 0.5 M 4-*tert*-butyl-pyridine, and 0.6 M 1,2-dimethyl-3-propylimidazolium iodide in dehydrated acetonitrile). The active area of the fiber-shaped DSC was calculated by multiplying the length and diameter of the working electrode.[7,10,16,17]

Acknowledgements

This work was supported by NSFC (91027025, 21225417), MOST (2011CB932503, 2011DFA51330), STCSM (11520701400, 12nm0503200), Fok Ying Tong Education Foundation, and the Program for Professor of Special Appointment at Shanghai Institutions of Higher Learning.

References

1 S. I. Na, S. S. Kim, J. Jo and D. Y. Kim, *Adv. Mater.*, 2008, **20**, 4061–4067.
2 J.-Y. Liao, B.-X. Lei, H.-Y. Chen, D.-B. Kuang and C.-Y. Su, *Energy Environ. Sci.*, 2012, **5**, 5750–5757.
3 Z. Yang, M. Liu, C. Zhang, W. W. Tjiu, T. Liu and H. Peng, *Angew. Chem., Int. Ed.*, 2013, **52**, 3996–3999.
4 F. Huang, D. Chen, L. Cao, R. A. Caruso and Y.-B. Cheng, *Energy Environ. Sci.*, 2011, **4**, 2803–2806.
5 L. Heng, X. Wang, N. Yang, J. Zhai, M. Wan and L. Jiang, *Adv. Funct. Mater.*, 2010, **20**, 266–271.
6 Z. Yang, T. Chen, R. He, G. Guan, H. Li, L. Qiu and H. Peng, *Adv. Mater.*, 2011, **23**, 5436–5439.
7 S. Zhang, C. Ji, Z. Bian, R. Liu, X. Xia, D. Yun, L. Zhang, C. Huang and A. Cao, *Nano Lett.*, 2011, **11**, 3383–3387.
8 C. Pan, W. Guo, L. Dong, G. Zhu and Z. L. Wang, *Adv. Mater.*, 2012, **24**, 3356–3361.
9 T. Chen, L. Qiu, Z. Yang and H. Peng, *Chem. Soc. Rev.*, 2013, **42**, 5031–5041.
10 Z. Lv, Y. Fu, S. Hou, D. Wang, H. Wu, C. Zhang, Z. Chu and D. Zou, *Phys. Chem. Chem. Phys.*, 2011, **13**, 10076–10083.
11 A. Hagfeldt, G. Boschloo, L. Sun, L. Kloo and H. Pettersson, *Chem. Rev.*, 2010, **110**, 6595–6663.
12 M. Grätzel, *Acc. Chem. Res.*, 2009, **42**, 1788–1798.
13 J. N. Clifford, E. Martínez-Ferrero, A. Viterisi and E. Palomares, *Chem. Soc. Rev.*, 2011, **40**, 1635–1646.
14 X. Liu, F. Wang and Q. Wang, *Phys. Chem. Chem. Phys.*, 2012, **14**, 7894–7911.
15 W. Wang, X. Sun, W. Wu, H. Peng and Y. Yu, *Angew. Chem.*, 2012, **124**, 4722–4725.
16 M. R. Lee, R. D. Eckert, K. Forberich, G. Dennler, C. J. Brabec and R. A. Gaudiana, *Science*, 2009, **324**, 232–235.
17 T. Chen, L. Qiu, H. G. Kia, Z. Yang and H. Peng, *Adv. Mater.*, 2012, **24**, 4623–4628.